(4)

CHEMICAL
RESEARCH,
DEVELOPMENT &
ENGINEERING
CENTER

CRDEC-TR-110

AEROSOL EXTINCTION TRANSMISSOMETRY AT VISIBLE AND INFRARED WAVELENGTHS APPLIED TO SPECIALIZED PROBLEMS IN CB DEFENSE

Hugh R. Carlon
U.S. Army Fellow
RESEARCH DIRECTORATE

October 1989

U.S. ARMY
ARMAMENT
MUNITIONS
CHEMICAL COMMAND

Aberdeen Proving Ground, Maryland 21010-5423

Disclaimer

The findings in this report are not to be construed as an official Department of the Army position unless so designated by other authorizing documents.

Distribution Statement

Approved for public release; distribution is unlimited.

UNCLASSIFIED
SECURITY CLASSIFICATION OF THIS PAGE

REPORT DOCUMENTATION PAGE

Form Approved
OMB No. 0704-0188

1a. REPORT SECURITY CLASSIFICATION UNCLASSIFIED	1b. RESTRICTIVE MARKINGS
2a. SECURITY CLASSIFICATION AUTHORITY	3. DISTRIBUTION / AVAILABILITY OF REPORT Approved for public release; distribution is unlimited.
2b. DECLASSIFICATION / DOWNGRADING SCHEDULE	
4. PERFORMING ORGANIZATION REPORT NUMBER(S) CRDEC-TR-110	5. MONITORING ORGANIZATION REPORT NUMBER(S)
6a. NAME OF PERFORMING ORGANIZATION CRDEC 6b. OFFICE SYMBOL (*If applicable*) SMCCR-RSP-P	7a. NAME OF MONITORING ORGANIZATION
6c. ADDRESS (*City, State, and ZIP Code*) Aberdeen Proving Ground, MD 21010-5423	7b. ADDRESS (*City, State, and ZIP Code*)
8a. NAME OF FUNDING / SPONSORING ORGANIZATION CRDEC 8b. OFFICE SYMBOL (*If applicable*) SMCCR-RSP-P	9. PROCUREMENT INSTRUMENT IDENTIFICATION NUMBER
8c. ADDRESS (*City, State, and ZIP Code*) Aberdeen Proving Ground, MD 21010-5423	10. SOURCE OF FUNDING NUMBERS PROGRAM ELEMENT NO.: PROJECT NO.: 1L161101 TASK NO.: A91A WORK UNIT ACCESSION NO.:

11. TITLE (*Include Security Classification*)
Aerosol Extinction Transmissometry at Visible and Infrared Wavelengths Applied to Specialized Problems in CB Defense

12. PERSONAL AUTHOR(S)
Carlon, Hugh R., U.S. Army Fellow

13a. TYPE OF REPORT	13b. TIME COVERED	14. DATE OF REPORT (*Year, Month, Day*)	15. PAGE COUNT
Technical	FROM 78 Jan TO 82 Dec	1989 October	40

16. SUPPLEMENTARY NOTATION

17 COSATI CODES			18. SUBJECT TERMS (*Continue on reverse if necessary and identify by block number*)
FIELD	GROUP	SUB-GROUP	Troposphere; Aerosol sampling; Aerosols; Mie theory; Electro-optics (continued on reverse)
07	04		
04	01		

19. ABSTRACT (*Continue on reverse if necessary and identify by block number*)

This report compiles, updates, and discusses several novel techniques in aerosol extinction transmissometry, in the visible and infrared wavelength regions, that are applicable to the solution of a variety of specialized problems in CB defense. These techniques share common elements with one another, and so they are brought together here for easy reference.

Complex calculations of optical scattering using high-speed electronic computers have become so commonplace that the technology has evolved into several specialty fields, e.g., extinction spectroscopy, angular scattering measurements and nephelometry. As a consequence, the overall technology and our ability to remotely characterize or quantitatively analyze atmospheric aerosols might be further advanced than is realized by workers in the individual disciplines who do not have the time to keep up with advances in other (continued on reverse)

20 DISTRIBUTION / AVAILABILITY OF ABSTRACT	21 ABSTRACT SECURITY CLASSIFICATION
☒ UNCLASSIFIED/UNLIMITED ☐ SAME AS RPT ☐ DTIC USERS	UNCLASSIFIED
22a. NAME OF RESPONSIBLE INDIVIDUAL SANDRA J. JOHNSON	22b TELEPHONE (*Include Area Code*) (301) 671-2914 22c. OFFICE SYMBOL SMCCR-SPS-T

DD Form 1473, JUN 86 *Previous editions are obsolete*

SECURITY CLASSIFICATION OF THIS PAGE
UNCLASSIFIED

18. Subject Terms (continued)

Nephelometry	Polarization
Atmosphere	Spheres
Optical scattering	Spectroscopy
Visible	Geometric regime
Lasers	Rayleigh regime
He:Ne	
Turbidity	
Infrared	

19. Abstract (continued)

disciplines. This report examines techniques of transmission (extinction) and turbidity spectroscopy, polarization and angular scattering measurements, and related developments and concludes that computer programs can be written to optimize desired parameters in interdisciplinary investigations. An appendix discusses sampling, which is a complicated problem in aerosol physics. A technique described to monitor continuously the mass concentration of monodisperse test aerosols using a He:Ne laser. Good approximations are possible from Mie theory. The method is fast, accurate, and eliminates the need for precalibration of a standard sampler to monitor aerosol mass concentration over increments of time. It can be used for sampler efficiency measurements and whenever it is desired to monitor test aerosols of spherical droplets continuously, e.g., in studies of the human respiratory system for droplets larger than a few micrometers. A second appendix discusses the estimation of mass extinction coefficients for nonabsorbing spherical aerosol particles in the geometric scattering regime. The techniques presented should find wide application in military electro-optical technology.

PREFACE

The work described in this report was authorized under Project No. 1L161101A91A, In-House Laboratory Independent Research (ILIR). This work was started in January 1978 and completed in December 1982. It was updated by reference to the recent open literature and prepared for publication in December 1988.

The use of trade names or manufacturers' names in this report does not constitute an official endorsement of any commercial products. This report may not be cited for purposes of advertisement.

This report has been approved for release to the public.

Acknowledgments

Significant contributions to the work described in the Appendixes of this report were made by David V. Kimball and Robert J. Wright, who carried out the laboratory investigations described, and by Robert Frickel and Merrill E. Milham, who performed many Mie calculations in support of this research. Bernard V. Gerber suggested the polarization and angular scattering studies that are described.

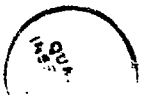

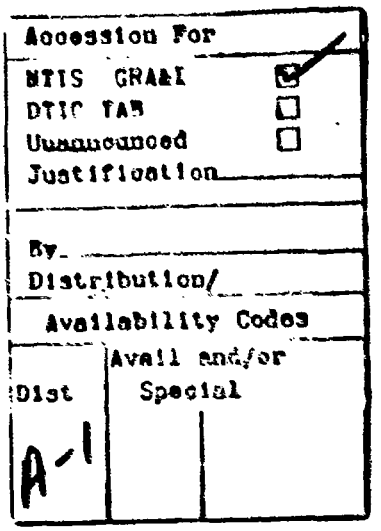

Blank

CONTENTS

LIST OF FIGURES

TABLE

AEROSOL EXTINCTION TRANSMISSOMETRY AT VISIBLE AND INFRARED WAVELENGTHS APPLIED TO SPECIALIZED PROBLEMS IN CB DEFENSE

1. INTRODUCTION AND BACKGROUND

With the increasing availability of high-speed electronic computers over the past two decades, complex calculations of optical extinction and scattering of electromagnetic radiation by atmospheric aerosols using the Mie theory[1] have become commonplace.

The technology has advanced so swiftly that specialists measuring, e.g., cloud extinction of aerosols often are unaware of advances being made simultaneously by other specialists measuring, e.g., angular scattering patterns of aerosols with nephelometers. Such measurements and calculations can be done in numerous wavelength regions, but the technology which concentrated first upon the visible wavelengths now is expanding rapidly especially into the regions of relatively high atmospheric transparency called "windows" in the infrared.

This technological expansion can be measured, for example, by a sampling of papers appearing one journal in one year alone, discussing aerosol measurements or calculations of extinction,[2-12] angular light scattering or nephelometry,[8,13-18] lidar,[19-22] and related aerosol technology including thermal emissivity[23] and calibration of optical particle counters.[24]

The author has noted several trends in all of this work. First, the utility and information content of simple extinction measurements has tended to be overlooked in the rush to exploit scattering techniques. Second, the polarization techniques do not seem to include applicable techniques, some new, that can be applied both to extinction and to polarization measurements. Third, that if taken in combination at this point in time, the overall technology might be further advanced than is realized by workers in the individual disciplines.

For example, remote characterization or quantitative analysis of tropospheric aerosols seems a distinct possibility, both by conventional transmission (extinction) spectroscopy and by angular scattering or backscattering techniques. This report examines these possibilities by first reviewing the technology of aerosol extinction spectroscopy.

The Beer-Lambert equation for atmospheric aerosols can be written:

$$- \ln T_\lambda = \alpha_\lambda C L, \qquad (1)$$

where for a given wavelength (μm), T_λ is the fractional transmittance, α_λ is the optical mass extinction coefficient of the aerosol (m^2g^{-1}), C is the aerosol mass concentration (g m^{-3}), and L is the optical path length (m). Some form of Equation (1) has been used by spectroscopists virtually since the birth of spectroscopy and the equation has become so well known that the power of simple extinction measurements of aerosols often is not fully appreciated.

For example, using suitable multi-wavelength techniques,[25,26] extinction measurements can contain sufficient information to allow direct determination of the mean size of a spherical droplet aerosol distribution,[27] or even remotely to characterize chemical reactions in cloud droplets at isosbestic wavelengths,[28] without the use of polarized radiation or other more sophisticated techniques.

It is not surprising, however, that polarization techniques have received heavy emphasis since their exploitation in the early 1940s to characterize military fog-oil smoke mean droplet diameters based, in part, in earlier work at the U.S. Bureau of Standards by Stratton and Houghton[29] using the Mie theory[1] that was first put forth in 1908 but had to await the availability of high-speed computers for exploitation.

Stratton and Houghton measured the polarization ratio only for transparent spheres for which, if the complex index of refraction m_λ is given by $(n - ik)_\lambda$ where n_λ is the real index and k_λ is the imaginary index (closely related to the absorption coefficient), then $k_\lambda = 0$.

Polarization measurements can be used to determine particle size distribution in addition to mean size of aerosol droplet distributions. This was recognized and the technique was developed in the 1960s. By 1969, Kerker and his co-workers[30-32] had extended the techniques of particle size distribution measurements to the extent discussed in his classical book on light scattering[33] that gives an excellent review of the technology as it existed then.

In recent years, there is an increased awareness that aerosol particle absorption, e.g., in the infrared where k_λ is not zero, can be interpreted in new ways using not only extinction measurements[25,27] or polarization measurements,[33] but the two together.[26] The author concurs that this is a promising field for new research.

2. AEROSOL EXTINCTION MEASUREMENTS

It is known that the variation of k_λ from values near zero in the visible wavelengths to significant ones in the infrared wavelengths provides a method for the determination of aerosol mean droplet size & mass concentration from simple extinction measurements if two or more wavelengths are selected properly for observation.

For example, at the He:Ne laser wavelength $\lambda = 0.63$ μm, k_λ is near zero and typical water fog droplets have diameters D_μ such that $D_\mu >> \lambda$ or, to use Kerker's criterion, the size parameter $\pi D_\mu/\lambda \geq 2.0$ so that the conditions for geometric scattering exist.

This leads to a constancy of the product $\alpha_\lambda . D_\mu \rightarrow 3.0\text{-}3.2$, where α_λ is defined in Equation (1). At the same time, the product $\alpha_\lambda . D_\mu$ decidedly is not constant with D_μ at wavelengths where k_λ is not equal to zero in the infrared. This is illustrated in Figure 1, calculated from the Mie theory.

In Figure 1, curves are shown for the infrared wavelengths of 8.5, 10.5 and 12.57 (or 4π) μm, as well as for a composite of wavelengths in the 8.5-12.57 μm region where extinction can be measured, e.g., by a simple broadband transmissometer operating at 8-13 μm in the atmospheric window region there.

While operation at a specific wavelength such as the 10.6 μm CO_2 laser line for comparison to a visible wavelength such as the He:Ne laser line at $\lambda = 0.63$ μm has advantages, a broadband infrared reference band also can be used. In fact, related findings using a filtered light source in the visible at $\lambda = 0.515$ μm and a 9-12 μm broadband transmissometer to study the formation and dissipation of water fogs were reported at least as early as 1970 by Carlon.[34]

When the techniques of Carlon, et al,[25,27] are extended to use the Mie theory to calculate functions of the transmittances T_λ at $\lambda = 0.63$ μm and the broadband or composite wavelength band 8.5-12.57 μm vs. water droplet diameter D_μ, curves like those shown in Figure 2 are obtained. It is seen that the curves are widely separated.

Thus, a sensitive method is provided for the determination of mean droplet diameter. Experimental points for a steam-generated water fog are shown in Figure 2; these give excellent agreement with calculated curves for example at $D_\mu = 8$ μm. This result was cited by Weinman, et al,[35] as approximating Deirmendjian's 1969 Model C-1 (or vice-versa),[36] where D_μ is taken as the mass median diameter.

What is uncertain is the kind of distribution to which this diameter is most applicable. Kerker[33] has given an informative discussion of particle size distributions, and of transmission (extinction) and turbidity measurements. In this report, turbidity can be taken as the product $\alpha_\lambda . C$ in Equation (1), having the units m^{-1}.

Justification for the use of a composite of wavelengths (Figure 1 and abscissa, Figure 2) can be found by examining calculated curves and steam-generated fog data points for the individual wavelengths $\lambda = 8.5$, 10.5 and 12.57 (or 4π) μm and plotting curves like Figure 2 as is done in Figure 3.

Viewing the plots from top to bottom in Figure 3, it can be seen that the fog data gave the best agreement with calculation for a mass median diameter (MMD) of 6 μm at $\lambda = 8.5$ μm, MMD = 10 μm at $\lambda = 10.5$ μm, and MMD = 6 μm at $\lambda = 4\pi$ μm

In his discussions of particle size distribution functions, Kerker[33] cautions that mean particle diameters obtained by using methods like those discussed in the present report may be adequate for most purposes if the distribution is sufficiently narrow, but strictly are valid only for monodisperse systems.

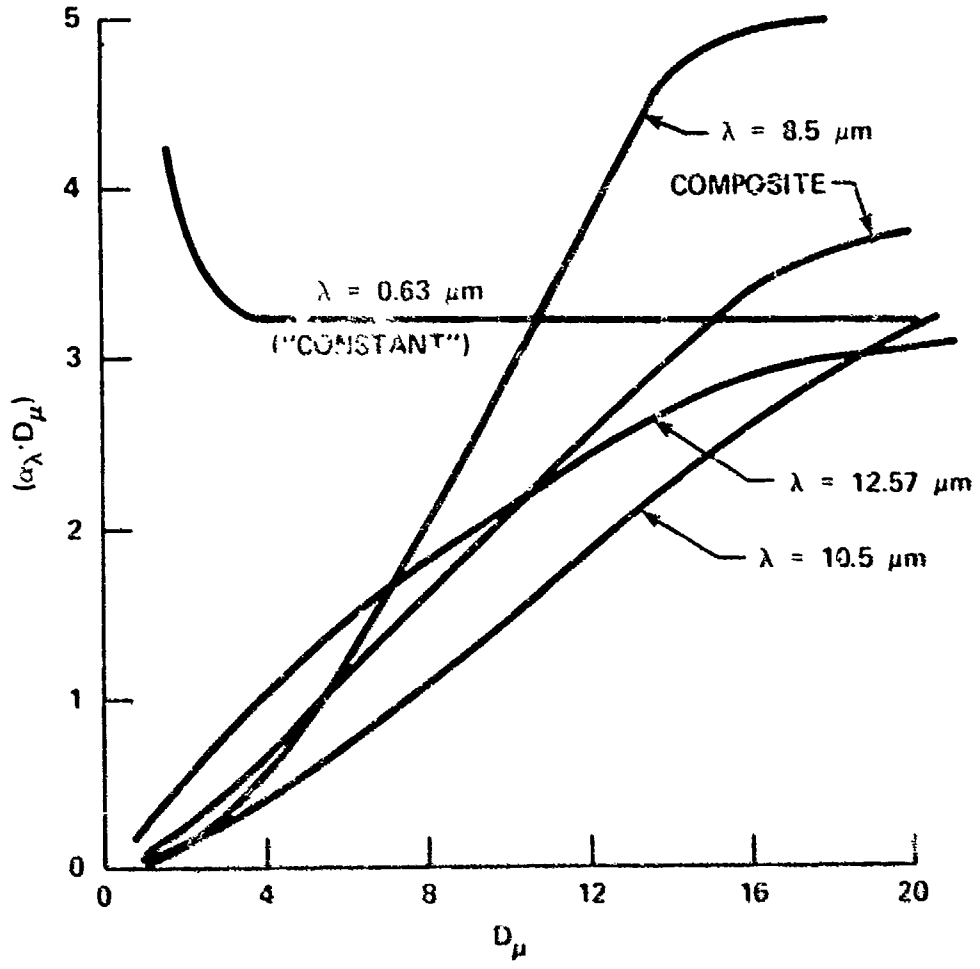

Figure 1. Values of $\alpha_\lambda . D_\mu$ vs D_μ Calculated From the Mie Program for Water; the "Constant" Function Actually is a Damped Oscillation.

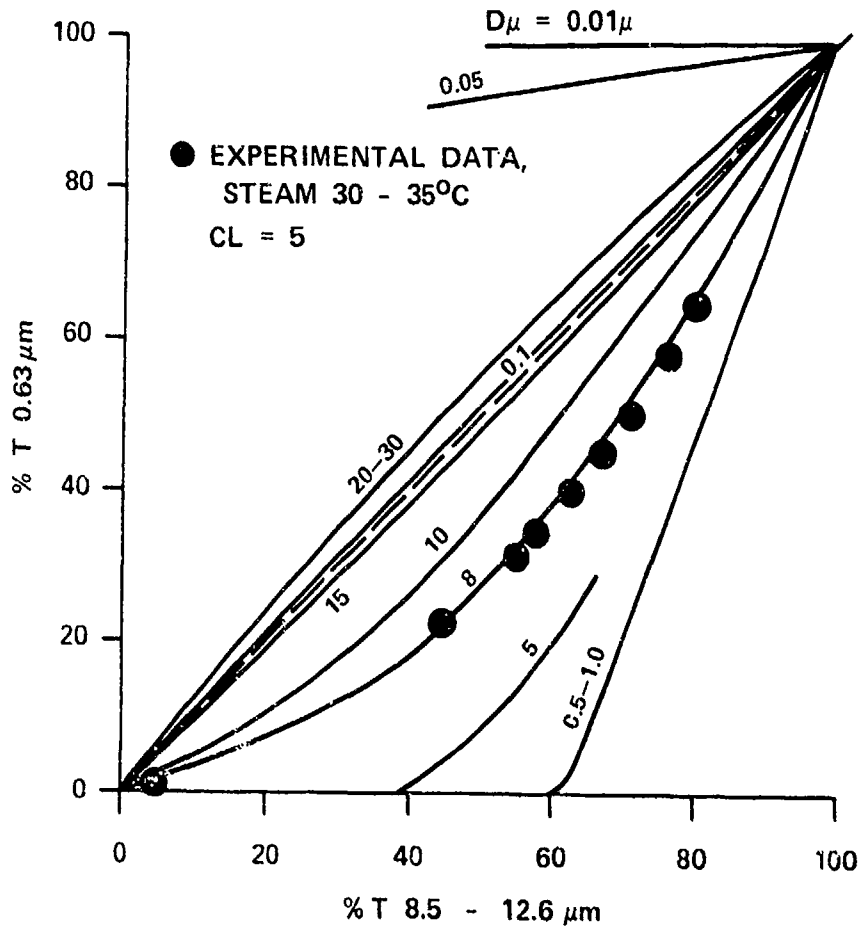

Figure 2. Comparison of Computed Curves Relating Visible to Infrared Optical Transmittance of Water Fog to Experimental Data Points for Cooling, Steam-Generated Water Fog Clouds.

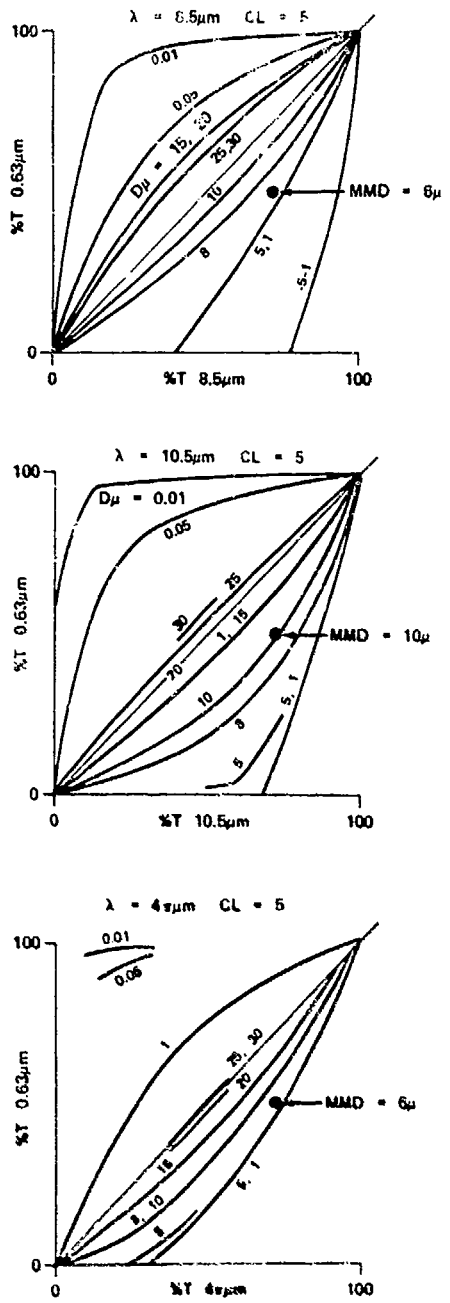

Figure 3. See Figure 2; Curves for Three Infrared Wavelengths Comprising the Broadband Composite of Wavelengths Shown as the Abscissa of Figure 2.

By using a composite of wavelengths to obtain a mean diameter, one is averaging both over wavelength intervals and over particle size distributions. But the results indicate that the technique works very well, especially under dynamic droplet growth or evaporation conditions where what is wanted most is a real-time indication of approximate droplet size, e.g. in studies of developing or dissipating water fogs.[34,37]

The dependence of α_λ upon λ is, in fact, highly variable due to variations in $(n - ik)_\lambda$, in addition to which α_λ varies with D_μ as was discussed previously. This is illustrated in Mie calculations for the extinction coefficient of water droplets (α_λ, ordinate) in Figure 4 vs D_μ for several wavelengths. At certain wavelengths, e.g., λ = 12.5 μm, the combined contributions of refractive (n_λ) and absorptive (k_λ) components of water droplet extinction lead to values of α_λ that virtually are independent of droplet size.

Experiments[27] seem to confirm for example that $\alpha_{12.5}$ is nearly constant with D_μ, suggesting that the liquid water content C in Equation (1) of a tropospheric optical path could be monitored by a simple 12.5 μm transmissometer with good precision for droplet sizes up to about 15 μm.[38] In this application, however, care must be taken to account for absorption due to hydrogen-bonded molecular clusters (water clusters) in the vapor leading to absorption easily confused with droplet absorption.[5]

At wavelengths called "isosbestic points",[28] the complex indices $(n - ik)_\lambda$ of some liquids are such that α_λ remains constant even though the liquid solutions comprising the droplet aerosol vary widely in their chemical composition, e.g., for droplets of orthophosphoric and related acids that might be formed by burning prosphorus in air of varying relative humidity (RH) such that solute (acid) concentrations vary from near zero to 85% by weight.

In Figure 5, λ = 11.4 μm is an isosbestic point calculated from refractive index measurements of pure orthophosphoric acid (H_3PO_4) in water.[39,40] Real atmospheric smokes obtained by burning phosphorus may contain mixtures of acids depending on rates of combustion in the presence of varying humidities and so may not give experimental spectra like those for pure H_3PO_4 in Figure 5 where $\alpha_{11.4}$ remains essentially constant at 0.13-0.15 m^2g^{-1}, while acid concentration varies from near zero to 85% by weight. This will be investigated.

Because of the constancy of $\alpha_{11.4}$ compared to the wide ranges of, say, $\alpha_{9.7}$ (see Figure 5) with solute concentration, remote characterization of the aerosol becomes a possibility if something is known about the droplet constituents. It can be shown that:

$$\alpha_\lambda \sim 4\pi k_\lambda f(m_\lambda)/\lambda\rho, \qquad (2)$$

where ρ (g cm^{-3}) is the droplet acid (solution) density, i.e., mass density, and:

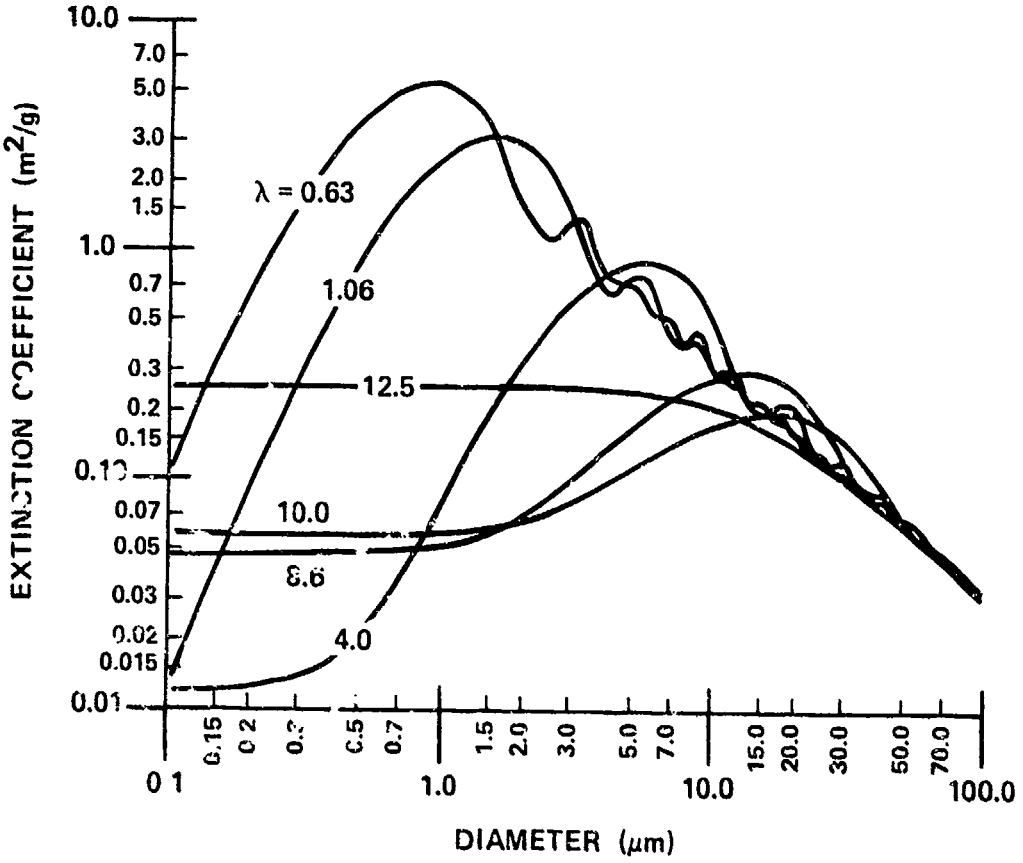

Figure 4. Calculated Curves for Water Droplets Showing α_λ vs D_μ; Note Constancy of $\alpha_{12.5}$ at All Wavelengths Up to About D_μ = 15 μm.

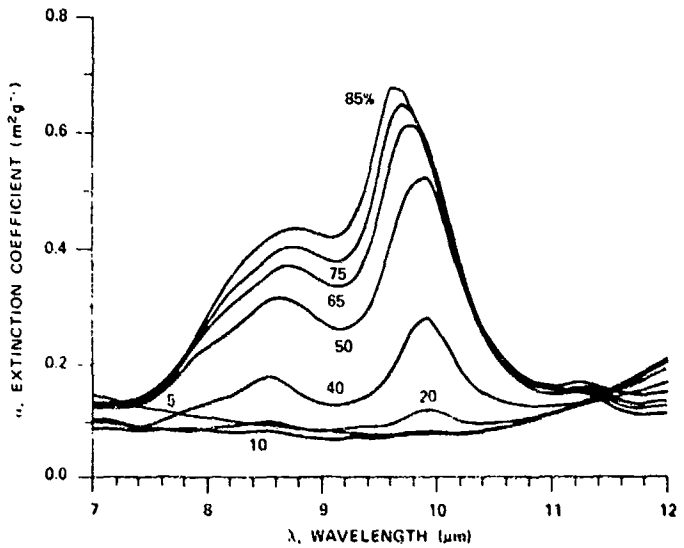

Figure 5. Computed Values of α_λ for Liquid Droplet Aerosols Comprising Several Concentrations of Orthophosphoric Acid (H_3PO_4) in Water.

$$f(m_\lambda) = \frac{9n_\lambda}{(n_\lambda^2 + k_\lambda^2)^2 + 4(n_\lambda^2 - k_\lambda^2) + 4} \qquad (3)$$

where $m_\lambda = (n - ik)_\lambda$ and the function of Equation 3 is plotted in Figure 6 for values of n_λ marked on the curves and ranging from 0.1 to 4.0, and for values of k_λ shown on the abscissa. It is emphasized that the above discussion applies to Rayleigh-scattering smokes where $D_\mu << \lambda$ as clearly is the case for orthophosphoric or other acid aerosols (smokes) produced by burning phosphorus in moist air.

Often it is useful to plot extinction coefficients or fractional transmittances vs D_μ rather than vs the size parameter $\pi D_\mu/\lambda$, for specific wavelengths. Two such calculated plots[41] are shown for water droplets in Figures 7 and 8. In Figure 7, the curves are calculated for a product C x L = 5.0 (Equation (1)) and for wavelengths, reading from top to bottom of the left-hand ends of the curves, of λ = 0.63, 8.5, 10.5 and 4π μm, i.e., the same wavelengths considered in Figures 1-3. In Figure 8, the curves are calculated for λ = 10 μm to show the functions vs D_μ of total extinction, and of the scattered and absorbed components that are summed to give total extinction, i.e.,

$$\alpha_T = \alpha_S + \alpha_A, \qquad (4)$$

where the subscripts indicate total (T), scattering (S), and absorptive (A) extinction.

Sassen[26] recognized that aerosol cloud extinction measured in conjunction with angular scattering measurements could lead to remote sensing of cloud composition by using two wavelengths like the laser wavelengths λ = 0.63 and 10.6 μm. But the present discussion indicates that such remote characterization could result from cloud extinction measurements alone at two closely-spaced infrared wavelengths, one of them an isosbestic point.

Additional data might be obtained by combining extinction and angular scattering measurements at an isosbestic wavelength. Optical parameters can carry only so much information, but the idea is provocative enough to warrant further investigation.

Other investigations of remote characterization of tropospheric aerosol clouds are possible, such as those based on effects peculiar to Christiansen wavelengths.[42] A complete discussion is given by Carlon,[4,5,42] where Reference 5 discusses aerosols ranging in size from molecular clusters to water cloud droplets.

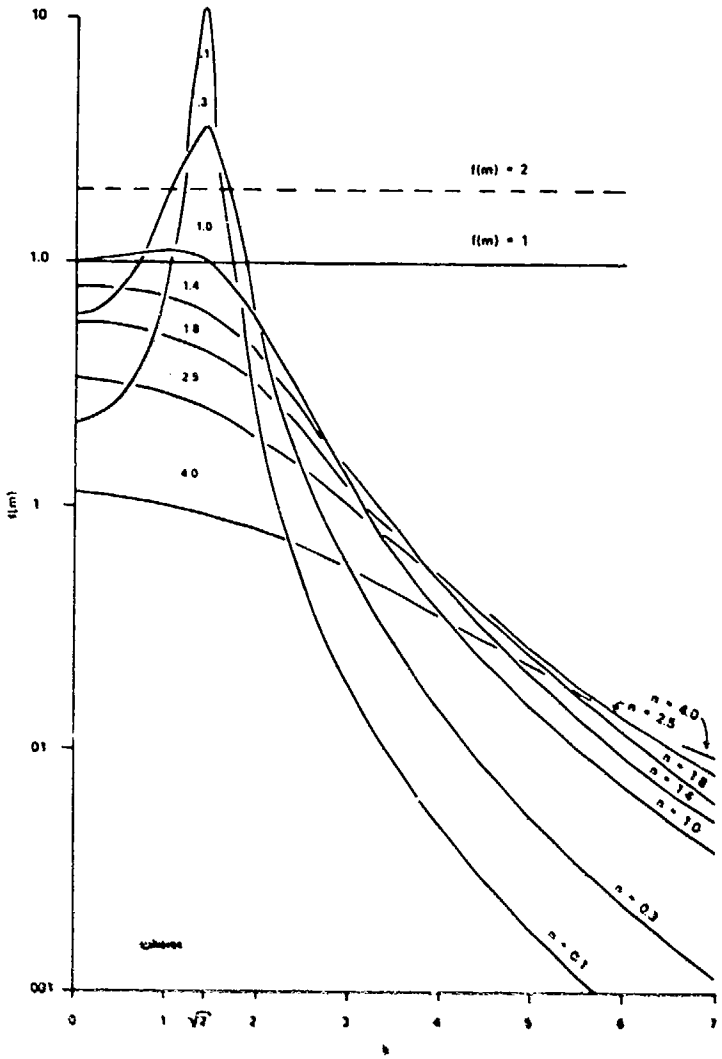

Figure 6. Plot of Equation (3) for n_λ values of 0.1-4.0 Shown on the Curves and κ_λ Values Shown on the Abscissa, for Rayleigh-Scattering Aerosols "Only".

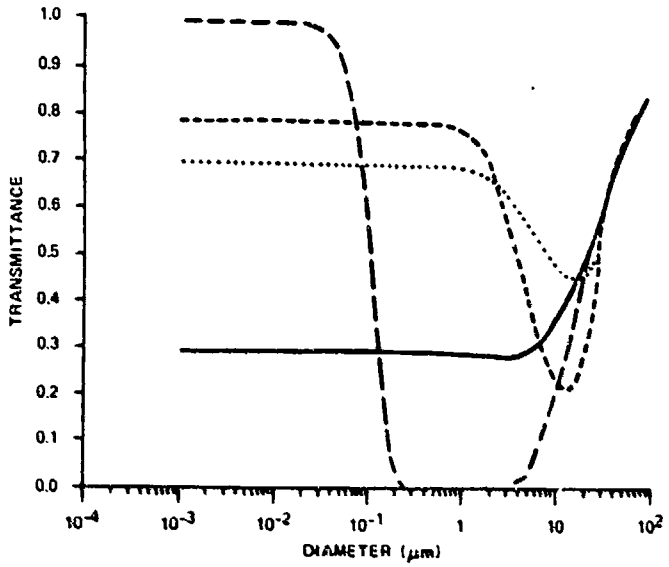

Figure 7. Fractional Transmittance for a C x L Product = 5 0 (Equation (1)) of Water Fog vs Droplet Diameter for Wavelengths, Reading from Top to Bottom of the Left-Hand Ends of the Curves, of λ = 0.63, 8.5, 10.5 and 4π μm, Which Are the Wavelengths Also Considered in Figures 1-3.

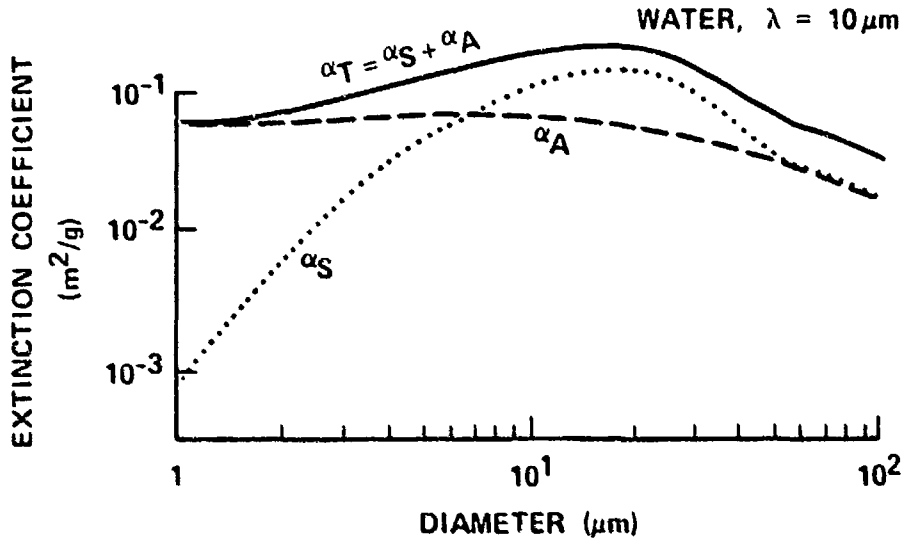

Figure 8. α_λ vs D_μ Calculated From the Mie Program at λ = 10μm for Water Droplets; the Subscripts T, S and A Refer to Ecuation (4).

3. POLARIZATION AND ANGULAR SCATTERING MEASUREMENTS

Kerker[33] has given an excellent review of techniques used to determine particle size distributions using measurements like these, and the present author will not elaborate except to raise a few pertinent points.

Sassen[26] verified that angular scattering patterns calculated from the Mie theory can be observed rather closely by experiment not only for spherical particles, but for irregularly-shaped ones as well. Thus polarization or angular scattering techniques combined with some of the recent advances in extinction measurement technology discussed here should provide new combinations for the remote characterization of tropospheric aerosols.

The polarization method[33] for evaluating the distribution of sphere sizes, utilizes polarization of scattered radiation obtained from a monochromatic light source at various angles of observation. The intensity of the components of the scattered light whose electric vector vibrates perpendicular and parallel to the plane of observation, $I_1(\theta)$ and $I_2(\theta)$, is measured at a number of angles, where θ is the scattering angle measured from the direction of the incident light beam. The polarization ratio, $P(\theta)$, is defined such that:

$$P(\theta) = I_2(\theta)/I_1(\theta). \qquad (5)$$

For example, $P(\theta)$ can be calculated as a function of θ for any assumed particle distribution such as the zeroth order logarithmic distribution (ZOLD) and for any standard deviation, σ_0, ranging from $\sigma_0 = 0$ (i.e., a monodisperse aerosol), to values of 0.3 or more where the curves flatten and the method approaches its limit of usefulness.

Figure 9 shows the family of curves calculated for the He:Cd laser wavelength $\lambda = 0.4416\ \mu m$, $D_\mu = 0.3\ \mu m$, $n_\lambda = 1.484$ and $k_\lambda = 0$ so that $m_\lambda = (1.484 - i.0)_\lambda$ and the density is $\rho = 0.98\ g\ cm^{-3}$. The curves are for dioctyl phthalate (DOP), a liquid that is commonly used for test aerosols.[6] Agreement between calculation and measurement using the polarization method is good to excellent, often within a few percent.

The effect of the wavelength of the monochromatic light upon the functions shown in Figure 9 is of special interest. This has been investigated[30,31] for visible and near-infrared wavelengths, including cases such as vanadium pentoxide (V_2O_5) for which strong absorption occurs at shorter visible wavelengths, i.e., where k_λ is not zero.[32]

From the discussion in the present report of special techniques using extinction measurements in the infrared where k_λ is not zero, it is suggested that combinations of visible and infrared wavelengths can optimize desired parameters using polarization techniques. Since the size parameter $\pi D_\mu/\lambda$ depends on wavelength, a change in the wavelength of the incident light will cause a shift in the position of the curve peaks in Figure 9 such that larger values of λ shift the peaks to the right.

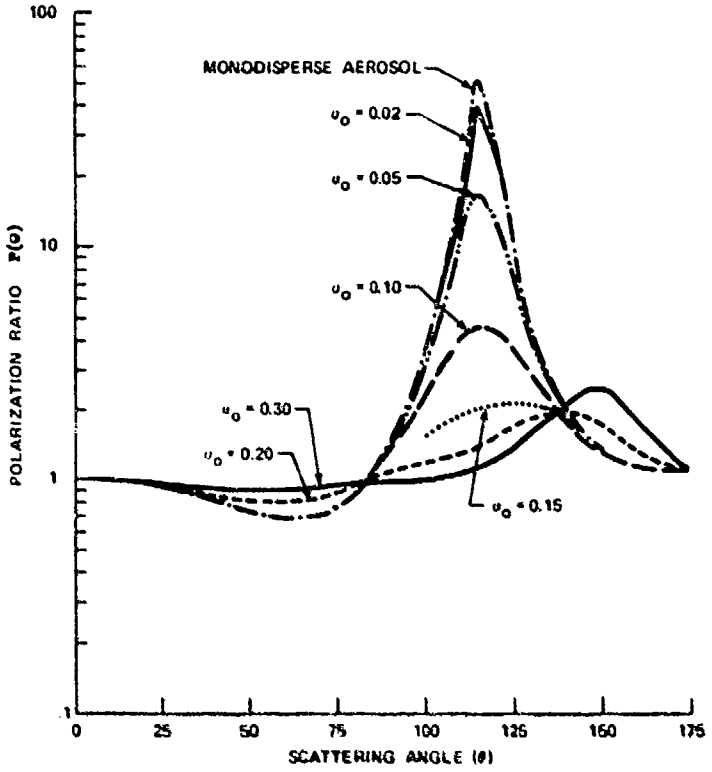

Figure 9. Polarization Ratio P(θ) vs Scattering Angle θ for DOP.

Multi-wavelength observations have been used to show that particle size distributions obtained at different wavelengths are consistent,[33] but when wavelength spacing is as great as λ = 0.63 and 10.5 μm additional work is needed to confirm this and also to determine whether the useful range of σ_o can be extended beyond 0.3 in measurements using the polarization method.

The scattering ratio method for the determination of particle size distribution is a variation where the angle of observation is held constant and the polarization ratio is measured or calculated over a spectrum or over a number of discete wavelengths.

The method was developed[43,44] in the early 1960s and was perfected by using monodisperse polystyrene latex spheres and known combinations of single sphere sizes to give mixtures of known size distributions checked by electron microscopy.

Thus the scattering ratio method gives an alternative way of studying, e.g., the variation of σ_o at some D_μ with λ at some constant θ, although the same thing can be done by using the polarization method directly and plotting, e.g., Figure 9 with λ as the abscissa at constant θ.

Turbidimetric particle size distribution methods invariably are similar to Wallach, et al.[46] Nelson[47] proposed a method by which calculated scattering cross sections from the Mie theory are compared to experimental extinction data using monodispersed polystyrene latex spheres in distilled water as a calibration means, and a computer program is used to null the error vs wavelength thus forcing a unique solution for the size distribution which is taken as bimodal to account for coagulation. The method also is said to yield particle volume concentration and the scattering cross section function, Q_λ. Extrapolation of the technique to tropospheric aerosols remains to be demonstrated.

4. SUMMARY AND CONCLUSIONS

This paper has concentrated on advances that have been made in the remote characterization of tropospheric aerosols by extinction and turbidimetric methods over the nearly two decades that have elapsed since the publication of Kerker's classic text.[33] The technology has been updated by including results not previously published with improved techniques in polarization and angular scattering methods. Perhaps most importantly, the author has tried to support the argument that if all methods presently available in this technology are taken into account at this time, our ability to remotely characterize or quantitatively analyze atmospheric aerosols is further advanced than workers in the individual light measurement disciplines realize.

It is concluded that by combinations of well-established and recently-developed light scattering techniques, investigators can undertake promising new areas of research. Some examples include combinations of extinction and polarization measurements with computer programs to study isosbestic or Christiansen wavelengths, and optimization of desired parameters as functions of wavelength or particle size distribution.

LITERATURE CITED

1. Mie, G., Ann. Phys. (Leipzig) 25, 377 (1908).

2. Carlon, H.R., "Contributions of Particle Absorption to Mass Extinction Coefficients (0.55-14 μm) of Soil-Derived Atmospheric Dusts," Appl. Opt. 19, 1165-1172 (1980).

3. Carlon, H.R., "Mass Extinction Coefficients Estimated for Non-Absorbing Spherical Aerosol Particles in the Geometric Scattering Regime," Appl. Opt. 19, 1891-1892 (1980).

4. Carlon, H.R., "Christiansen Effect in Infrared Spectra of Soil-Derived Atmospheric Dusts: Addenda," Appl. Opt. 19, 1892 (1980).

5. Carlon, H.R., "Aerosol Spectrometry in the Infrared," Appl. Opt. 19, 2210-2218 (1980).

6. Carlon, H.R., Kimball, D.V., and Wright, R.J., "Laser Monitoring of Mass Concentrations of Monodisperse Test Aerosols," Appl. Opt. 19, 2366-2369 (1980).

7. Bruce, C.W., Yee, Y.P., and Jennings, S.G., "In Situ Measurement of the Ratio of Aerosol Absorption to Extinction Coefficient," Appl. Opt. 19, 1893-1894 (1980).

8. Tam, W.G., and Zardecki, A., "Off-Axis Propagation of a Laser Beam in Low Visibility Weather Conditions," Appl. Opt. 19, 2822-2827 (1980).

9. Tam, W.G., "Multiple Scattering Corrections for Atmospheric Aerosol Extinction Measurements," Appl. Opt. 19, 2090-2092 (1980).

10. Janzen, J., "Extinction of Light by Highly Nonspherical Strongly Absorbing Colloidal Particles: Spectrophotometric Determination of Volume Distributions for Carbon Blacks," Appl. Opt. 19, 2977-2985 (1980).

11. Yue, G.K., and Deepak, A., "Modeling of Growth, Evaporation and Sedimentation Effects on Transmission of Visible and IR Laser Beams in Artificial Fogs," Appl. Opt. 19, 3767-3774 (1980).

12. Ariessohn, P.C., Self, S.A., and Eustis, R.H., "Two-Wavelength Laser Transmissometer for Measurements of the Mean Size and Concentration of Coal Ash Droplets in Combustion Flows," Appl. Opt. 19, 3775-3781 (1980).

13. Wyatt, P.J., "Some Chemical, Physical, and Optical Properties of Fly Ash Particles," Appl. Opt. 19, 975-983 (1980).

14. Kapustin, V.N., Rozenberg, G.V., Ahlquist, N.C., Covert, D.S., Waggoner, A.P., and Charlson, R.J., "Characterization of Nonspherical Atmospheric Aerosol Particles with Electrooptical Nephelometry," Appl. Opt. 19, 1345-1348 (1980).

15. Weil, H., and Chu, C.M., "Scattering and Absorption by Thin Flat Aerosols," Appl. Opt. 19, 2066-2071 (1980).

16. Horvath, H., "Determination of the Scattering Function of Atmospheric Aerosols with a Telephotometer," Appl. Opt. 19, 2651-2652 (1980).

17. Hansen, M.Z., and Evans, W.H., "Polar Nephelometer for Atmospheric Particulate Studies," Appl. Opt. 19, 3389-3395 (1980).

18. Hanzen, M.Z., "Atmospheric Particulate Analysis Using Angular Light Scattering," Appl. Opt. 19, 3441-3448 (1980).

19. Gardner, C.S., Sechrist, C.F., Jr., and Shelton, J.D., "Lidar Observations of the Mount Saint Helens Dust Layers Over Urbana, Illinois," Appl. Opt. 19, A192-3031 (15 Sep, 1980).

20. Randhawa, J.S., and Van der Laan, J.E., "Lidar Observations During Dusty Infrared Test-1," Appl. Opt. 19, 2291-2297 (1980).

21. Schuster, B.G., and Kyle, T.G., "Pollution Plume Transport and Diffusion Studies Using Fluorescence Lidar," Appl. Opt. 19, 2524-2528 (1980).

22. Carswell, A.I., and Pal, S.R., "Polarization Anisotropy in Lidar Multiple Scattering From Clouds," Appl. Opt. 19, 4123-4126 (1980).

23. Walker, P.L., "Thermal Emissivity of a Polydisperse Aerosol Medium," Appl. Opt. 19, 2271 (1980).

24. Jeck, R.K., "Calibration and Testing of Optical Single-Particle-Size Spectrometers with Monofilament Fibers as Substitute Particles," Appl. Opt. 19, 657-658 (1980).

25. Carlon, H.R., Milham, M.E., and Frickel, R.H., "Determination of Aerosol Droplet Size and Concentration from Simple Transmittance Measurements," Appl. Opt. 15, 2452-2456 (1976).

26. Sassen, K., "Infrared (10.6 μm) Scattering and Extinction in Laboratory Water and Ice Clouds," Appl. Opt. 20, 185-193 (1981).

27. Carlon, H.R., Anderson, D.H., Milham, M.E., Tarnove, T.L., Frickel, R.H., and Simoni, I., "Infrared Extinction Spectra of Some Common Liquid Aerosols," Appl. Opt. 16, 1598-1605 (1977).

28. Carlon, H.R., "Isosbestics in Infrared Aerosol Spectra: Proposed Applications for Remote Sensing," Infrared Phys. 21, 93-99 (1981).

29. Stratton, J.A., and Houghton, H.G., "A Theoretical Investigation of the Transmission of Light Through Fog," Phys. Rev. 38, 159-165 (1931).

30. Kerker, M., Matijevic, E., Espenscheid, W.F., Farone, W.A., and Kitani, S., "Aerosol Studies by Light Scattering I. Particle Size Distribution by Polarization Ratio Method," J. Colloid Sci. 19, 213-222 (1964).

31. Espenscheid, W.F., Matijevic, E., and Kerker, M., "Aerosol Studies by Light Scattering. III. Preparation and Particle Size Analysis of Sodium Chloride Aerosols of Narrow Size Distribution," J. Phys. Chem. 68, 2831-2842 (1964).

32. Jacobsen, R., and Kerker, M., "Optical Properties of Vanadium Pentoxide," J. Opt. Soc. Amer. 57, 751-755 (1967).

33. Kerker, M., The Scattering of Light and Other Electromagnetic Radiation, Academic Press, New York, 1969.

34. Carlon, H.R., "Infrared Emission by Fine Water Aerosols and Fogs," Appl. Opt. 9, 2000-2006 (1970).

35. Weinman, J.A., Harshvardhan, and Olsen, W.S., "Infrared Radiation Emerging From Smoke Produced by Brush Fires," Appl. Opt. 20, 199-206 (1981).

36. Deirmendjian, D., Electromagnetic Scattering on Spherical Polydispersions, Elsevier, New York, 1969.

37. Carlon, H.R., and Shaffer, R.E., "Optical Properties (0.63-13 μm) of Water Fogs Stabilized Against Evaporation by Long-Chain Alcohol Coatings," J. Colloid Interface Sci. 82, 203-207 (1981).

38. Carlon, H.R., "Apparatus and Method for Measuring Liquid Water Content of A Cloud or Fog," U.S. Patent 4,154,089, 1979.

39. Querry, M.R., Tyler, I.L., and Holland, W.E., Bull. Am. Phys. Soc. 22, 641 (1977).

40. Querry, M.R., and Tyler, I.L., "Complex Refractive Indices in the Infrared for H_3PO_4 in Water," J. Opt. Soc. Am. 68, 1404 (1978).

41. Hale, G.M., and Querry, M.R., "Optical Constants of Water in the 200-nm to 200-μm Wavelength Region," Appl. Opt. 12, 555-563 (1973).

42. Carlon, H.R., "Christiansen Effect in Infrared Spectra of Soil-Derived Atmospheric Dusts," Appl. Opt. 18, 3610-3614 (1979).

43. Stevenson, A.F., Heller, W., and Wallach, M.L., "Theoretical Investigations on the Light Scattering of Colloidal Spheres. XI. Determination of Size Distribution Curves from Spectra of the Scattering Ratio or from Depolarization Spectra," J. Chem. Phys. 34, 1789-1795 (1961).

44. Heller, W., and Wallach, M.L., "Experimental Investigations on the Light Scattering of Colloidal Spheres. V. Determination of Size Distribution Curves by Means of Spectra of the Scattering Ratio," J. Phys. Chem. 67, 2577-2583 (1963).

45. Wallach, M.L., and Heller, W., "Experimental Investigations on the Light Scattering of Colloidal Spheres. VI. Determination of Size Distribution Curves by Means of Turbidity Spectra," J. Phys. Chem. 68, 924-930 (1964).

46. Wallach, M.L., Heller, W., and Stevenson, A.F., "Theoretical Investigations on the Light Scattering of Colloidal Spheres. XII. The Determination of Size Distribution Curves from Turbidity Spectra," J. Chem. Phys. 34, 1796-1802 (1961).

47. Nelson, H.F., "Radiative Scattering Cross Sections: Comparison of Experiment and Theory," Appl. Opt. 20, 500-504 (1981).

APPENDIX A

LASER MONITORING OF MASS CONCENTRATIONS OF MONODISPERSE TEST AEROSOLS

A1. INTRODUCTION

Aerosol sampling usually is considered to be a very complicated problem[A1] in aerosol physics. It may be desired, for example, to determine the efficiency, as a function of particle diameter D_μ (μm), with which aerosol particles of various kinds are drawn into an aspirated sampling tube or head or into the human respiratory system.

The principal experimental difficulty is one of establishing and maintaining a test aerosol of known characteristics, including composition, mass or number concentration, and particle size distribution. The aerosol sampler is placed in the test aerosol and is operated at a known flow rate for a known period of time, after which a determination is made, usually by weighing a filter paper in the sampler, of the mass of the collected aerosol. This is ratioed to the particle mass contained in the sampled volume of the test aerosol to determine the sampler efficiency.

The problem of maintaining the test aerosol is not a trivial one. It must be sampled periodically to determine if (and how) it is changing with time as, for example, particles settle or agglomerate. This sampling disturbs and draws material from the test aerosol, and the subsequent analyses usually require at least several minutes to complete, during which period the characteristics of the test aerosol may continue to change.

This appendix describes a technique by which the test aerosol mass concentration is continuously sampled by a laser beam. This requires that the optical constants, particle size distribution, and other properties of the aerosol particles be known. The test aerosol materials discussed in this paper are liquids that are generated as spherical droplets, for which accurate (+ or - 10%) optical calculations can be made using the Mie theory.[A2]

For approximation purposes in optical calculations, it is often useful to treat an aerosol as if it consisted entirely of monodisperse particles of some equivalent diameter.[A3] But a better approach is to generate monodisperse droplet aerosols directly, as was done in the work reported here.

A2. THEORY

In the geometric optical scattering regime, particle diameters are much larger than the wavelength λ (μm) of observation. That is, $D_\mu \gg \lambda$. Under these conditions, it is straightforward to show[A4] that:

$$\alpha_\lambda = 3Q_\lambda / 2D_\mu \rho \qquad (A1)$$

where α ($m^2 g^{-1}$) is the mass extinction coefficient of the spherical particles, ρ (g cm^{-3}) is the particle density, and Q_λ is the cross-section efficiency factor, which is very nearly constant and equal to 2.0 for the liquid aerosol droplets discussed in this paper,[A3] so that:

$$\alpha_\lambda \sim 3/D_\mu \rho \qquad (A2)$$

The mass extinction coefficient is used in the Beer-Lambert equation:

$$- \ln T_\lambda = \alpha_\lambda C L, \qquad (A3)$$

where T_λ is the optical transmittance at laser wavelength λ, C (g m^{-3}) is the aerosol mass concentration, and L is the optical path length uniformly filled by the aerosol (m). C, the quantity sought for the test aerosol, is then:

$$C = - \frac{1}{\alpha_\lambda L} \ln T_\lambda \sim - \frac{D_\mu \rho}{3 L} \ln T_\lambda \qquad (A4)$$

Several liquids used to generate test aerosols in work described in this appendix are shown in the table.

Table. Liquids Used to Generate Test Aerosols

Symbol	Substance	ρ, density, (g/cm^3)	Temperature (°C)	Real index* (n_D)
DMP	o-Dimethyl phthalate	1.192	20.8	1.5155
DEP	o-Diethyl phthalate	1.12	17.7	1.5029
DBP	n-Dibutyl phthalate	1.045	25.0	1.4925
DOP	Dioctyl phthalate	0.98	20.0	1.4590

* The sodium D line is at the 0.589-μm wavelength, and the real index at the He-Ne laser wavelength of 0.63 μm is nearly identical to this value for transparent colorless liquids.

Mie calculations were performed for the He:Ne laser (λ = 0.63 μm), with results as shown in Figure A1, and it was confirmed that the approximation of Equation (A2) is quite precise, i.e., that the functional dependence of $\alpha_{0.63}$, the extinction coefficient, on D_μ is very similar for all liquid aerosol materials considered, with only liquid densities ρ having a predictable effect.

The laser wavelength (0.63 μm) lies very close to the sodium D line (0.589 μm), and the materials listed in Table A1 are transparent and colorless in the visible wavelengths (i.e., they have a real refractive index n but a negligible absorption coefficient or imaginary index k). Thus it was very convenient to obtain the real indices of these materials using a standard laboratory refractometer at the sodium D line and to use these in Mie calculations for the 0.63-μm wavelength. The error introduced by doing this is very small, as is indicated by Figure A2, which compares the α_λ vs D_μ functions for DMP calculated at λ = 0.589 and 0.63 μm.

After preliminary testing, it was found convenient to use the liquid DOP (Figure A3) in most subsequent work. Since ρ = 0.98 g cm^{-3} for DOP, the approximations in Equations (A2) and (A4) can be still further simplified:

$$\alpha_{0.63} \sim 3/D_\mu, \tag{A5}$$

and:

$$C \sim -\frac{D_\mu}{3L} \ln T_{0.63} \tag{A6}$$

It can be seen from Figure A3 that the approximation of Equation (A5) is quite precise in the geometric regime ($D_\mu \gg \lambda$).

A3. EXPERIMENTAL PROCEDURE

A 1-m^3 test chamber was constructed and used as shown schematically in Figure 4. The He:Ne laser was optically aligned through pinholes in opposite chamber walls. The pinholes were utilized to prevent window effects. A pressure-equalization scheme between the chamber interior and room air prevented aerosol particles from flowing in either direction through the pinholes during testing.

Although Figure 4 shows an aerosol cloud coming from the generator, the chamber was stirred during testing to ensure uniform mixing. This was important because laser path length L of the laser beam in the test chamber (which was 1 m long) must be filled uniformly with the test aerosol during measurements.

The aerosol generator was of the spinning disk design[A5] to produce essentially monodisperse liquid droplets of test aerosol. The droplet size D_μ disseminated by the spinning disk generator is determined by the diameter and angular velocity of the disk, by the liquid flow rate, and to a lesser extent by other parameters including temperature.

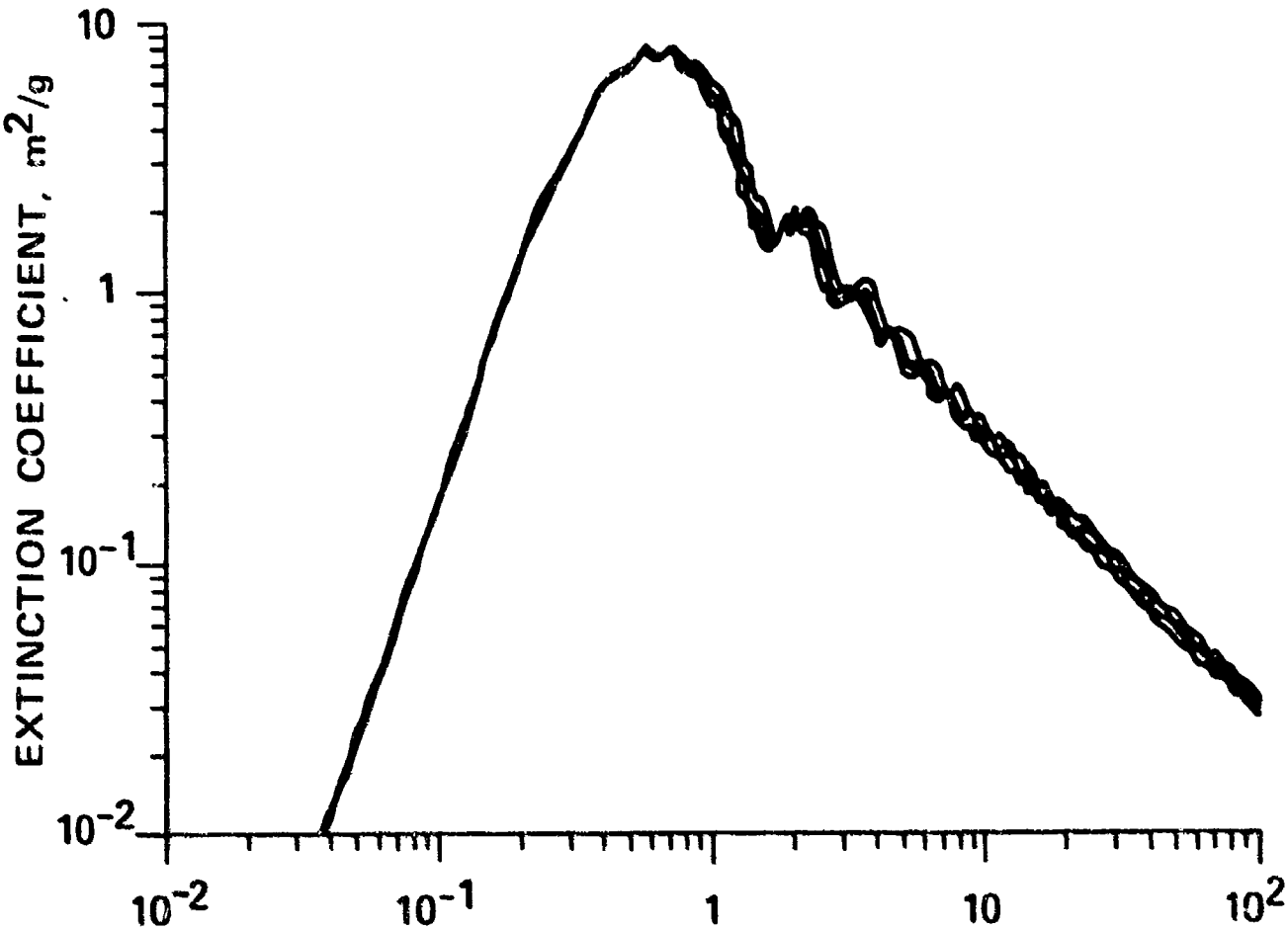

Figure A1. Values of $\alpha_{0.63}$ vs D_μ Calculated From the Mie Theory for Liquids Listed in Table A1.

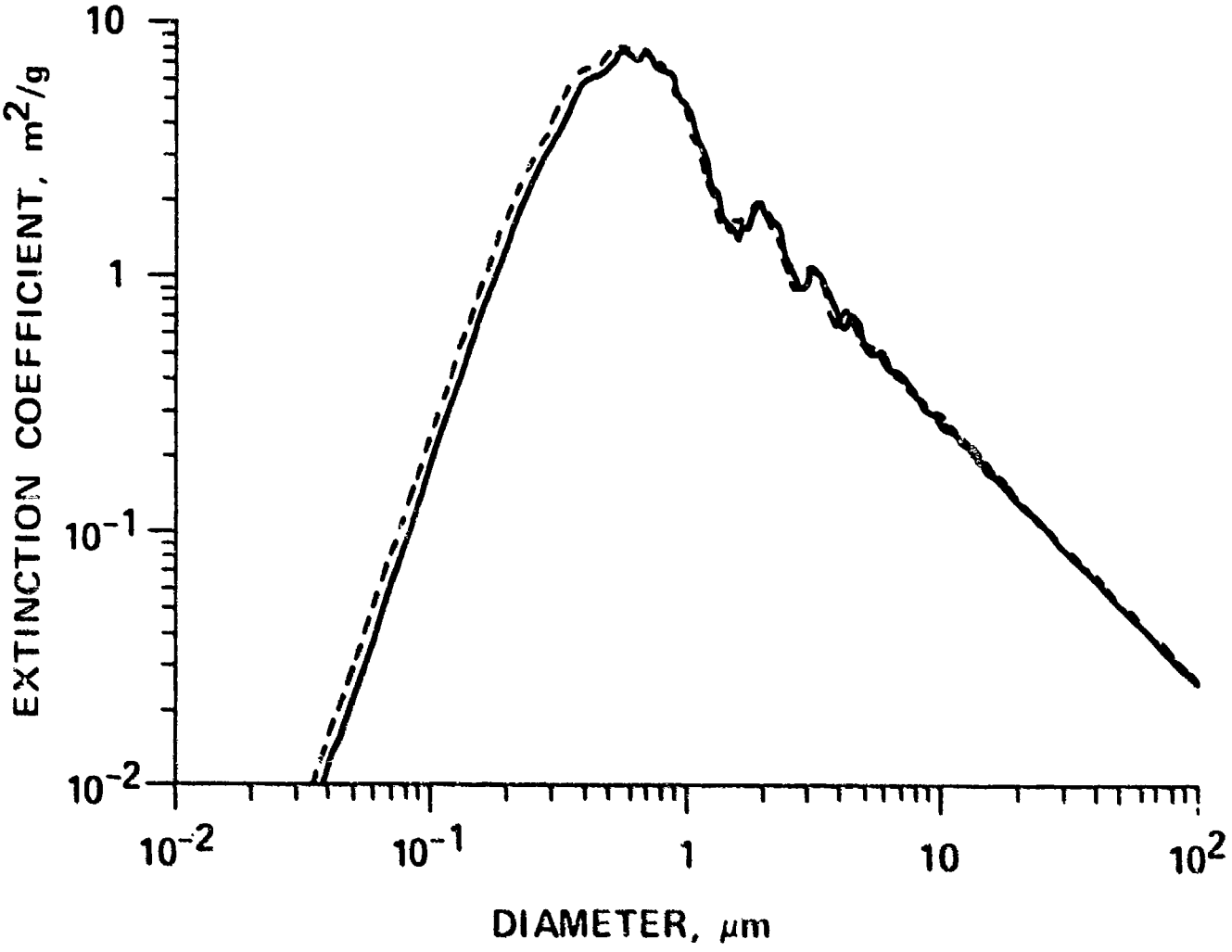

Figure A2. Values of α_λ vs D_μ Calculated From the Mie Theory for Dimethyl Phthalate (DMP), Using the Sodium D Line Refractive Index Measured at Its Wavelength of 0.589 μm (Dashed Curve) and Assuming the Same Index at the He:Ne Laser Wavelength λ = 0.63 μm (Solid Curve).

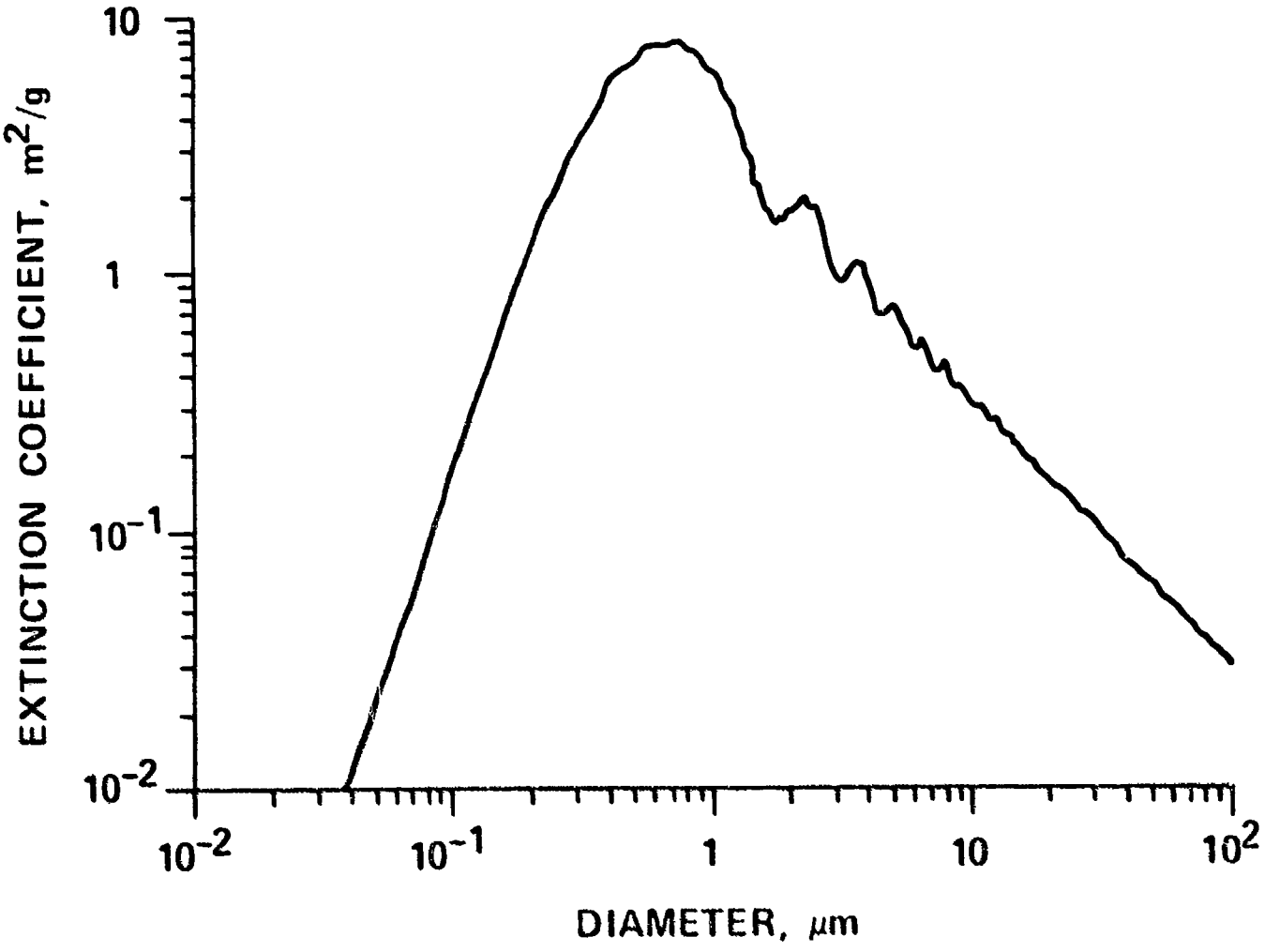

Figure A3. Values of $\alpha_{0.63}$ vs D_μ Calculated From Mie Theory for Dioctyl Phthalate (DOP).

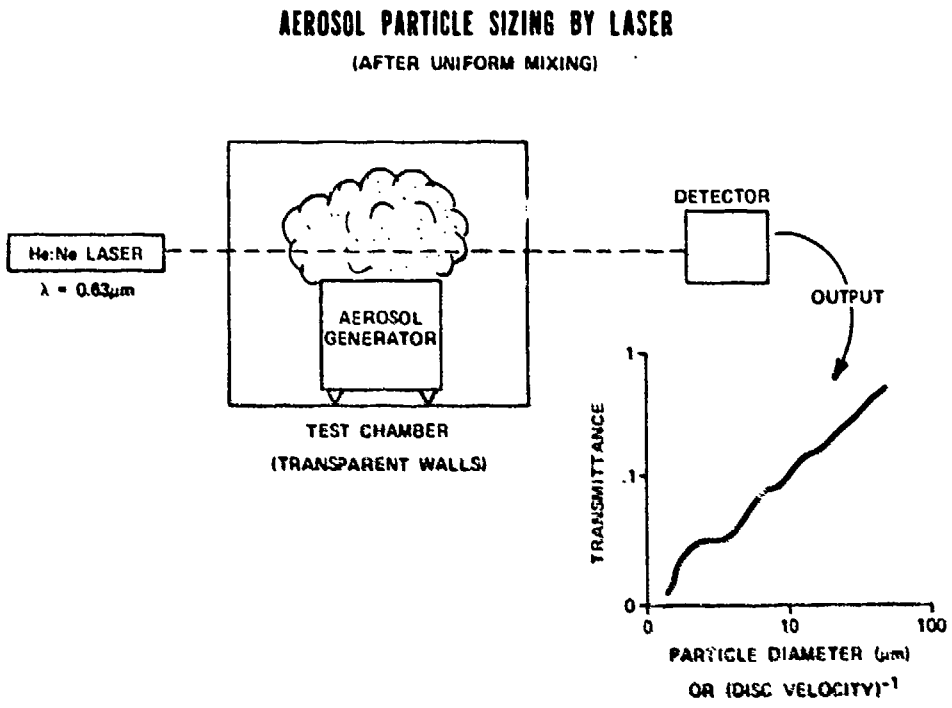

Figure A4. Schematic Representation of the Experimental Setup; the Chamber Was Stirred to Ensure Uniform Aerosol Mixing in the Laser Beam.

Aerosol droplet size was checked by microscopic examination of samples deposited on glass slides. The generator was easily capable of disseminating mass concentrations of test aerosols in the range C = 0.1-1.0 g m^{-3} for these tests. Other monodisperse aerosol generators are commercially available, although some* do not have the aerosol output capability of the unit used in these tests. Plastic microspheres** also were used in some trials, for which the $\alpha_{0.63}$ vs D_μ functions were not much different from those shown in Figure A1.

For testing, aerosol samplers were mounted completely inside the chamber with their inlets positioned perpendicular to and directly adjacent to the laser beam. This ensured that the laser beam and inlets intercepted identical samples. A refinement to this procedure involves using a second laser beam perpendicular to the first and nearly intersecting it, thus providing laser beam "cross hairs", which can be positioned directly in front of the sampler inlet tube under test.

A4. RESULTS AND DISCUSSION

The purpose of this appendix is to describe a technique by which the mass concentration of a sized test aerosol can be continuously sampled by a laser beam to improve experimental procedures. Only a brief discussion of typical test data for aspirated sampler efficiencies will be given here. Figure A5 presents some data for DOP droplets and illustrates the methodology discussed in this paper.

In Figure A5, the solid and dashed curves labeled Aspirated Sampler ae typical of the efficiencies measured. For these aspirated samplers, the sampling efficiency falls to less than 10% in the DOP droplet size range D_μ = 30-40 μm. The He:Ne laser can be considered 100% efficient in sampling the test aerosol, since laser attenuation depends entirely on extinction by the aerosol droplets (e_L = 100%).

Multiple scattering of the laser beam is not a problem, since the test aerosol concentration is always chosen to give high transmittances (0.7-1.0), thus conserving the aerosol material. The assumption that the actual mass concentration of the test aerosol, C_{actual}, is equal to that determined from the laser using Equation (A6), C_{laser}, is valid to within the error of the Mie calculations, which was found to be as good as plus or minus 10% in this application.

The equivalent mass concentration collected by the aspirated sampler, $C_{sampled}$, is determined by weighing the filter paper in the sampler before and after an aerosol trial and is reproducible within about plus or minus 10%. The percent efficiency of the sampler e_S is then 100 x ($C_{sampled}/C_{actual}$). When the test aerosol particle diameter is only

---

* The Berglund-Liu monodisperse aerosol generator is marketed by Thermo-Systems, Inc. (TSI), P.O. Box 3394, St. Paul, Minnesota 55165.

** Microspheres of glass, polystyrene, and other materials are available from Duke Scientific Corp., 445 Sherman Avenue, Palo Alto, Calif. 94306.

DETERMINATION OF ASPIRATED SAMPLER EFFICIENCY USING LASER BEAM

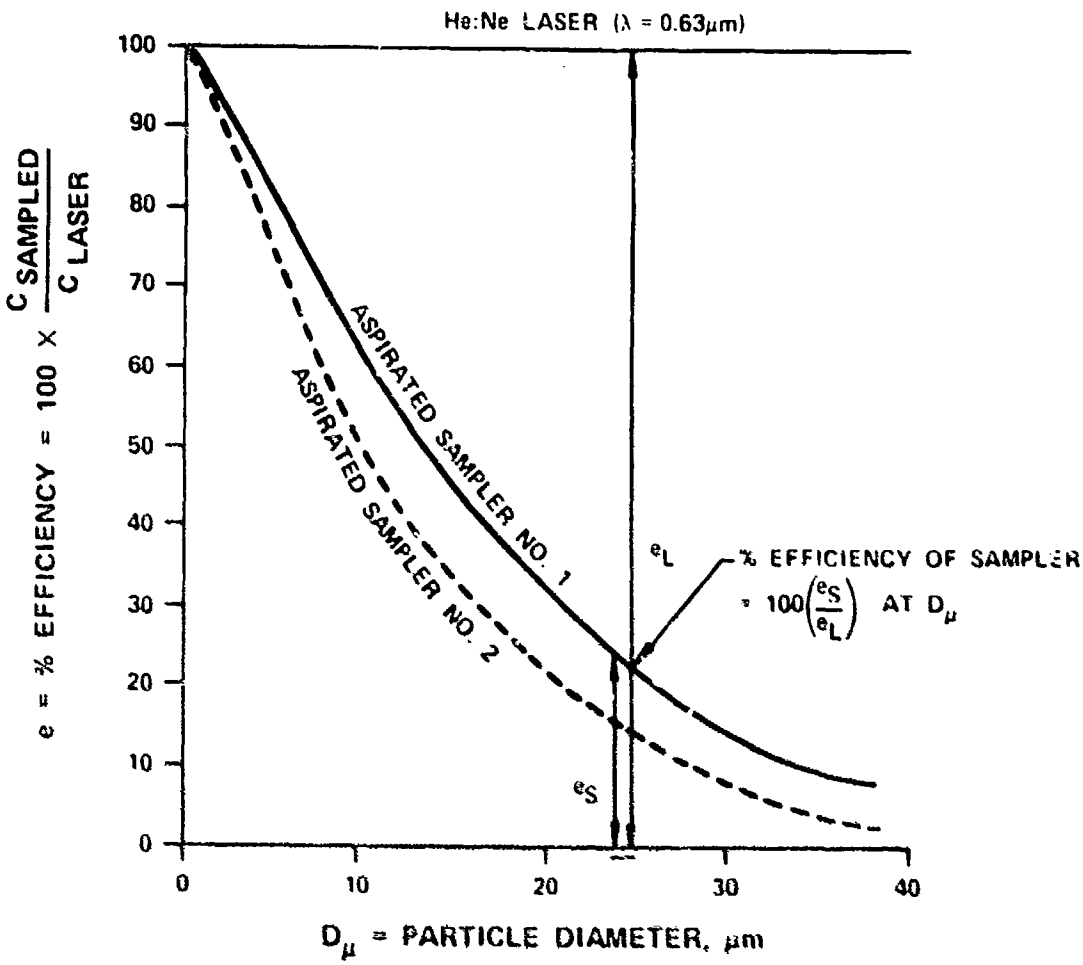

Figure A5. Typical Sampling Efficiencies for DOP Test Aerosols Are Shown by the Curves; the Methodology of Measurements Also Is Illustrated.

a few micrometers or less, the aspirated sampler efficiency approaches 100%, and these samplers can be used directly to confirm laser measurements of aerosol mass concentration as was reported previously for smoke aerosols.[A6]

A5. CONCLUSIONS

The discussion in this appendix has been limited to the determination of aspirated aerosol sampler efficiencies using laser reference techniques. These techniques, of course, are not limited to sampler efficiency measurements but can be used wherever it is desirable to continuously monitor the mass concentration of a test aerosol of spherical droplets, e.g., in studies of the human respiratory system.

By using a He:Ne laser in the visible wavelengths (λ = 0.63 μm), aerosol measurements are made in the geometric scattering regime (D_μ λ) using materials for which many simplifications and precise approximations are possible from the Mie theory. The method is fast, accurate, and eliminates the need for precalibration of standard samplers against which, for example, candidate samplers must be compared.

LITERATURE CITED

A1. Davies, C.N., The Entry of Aerosols into Sampling Tubes and Heads," Brit. J. Appl. Phys. (J. Phys. D) 1, 921-932 (1968).

A2. Mie., G., Ann. Phys. (Leipzig) 25, 377 (1908).

A3. Carlon, H.R., Milham, M.E., and Frickel, R.H., "Determination of Aerosol Droplet Size and Concentration from Simple Transmittance Measurements," Appl. Opt. 15, 2452-2456 (1976).

A4. Carlon, H.R., "Practical Upper Limits of the Optical Extinction Coefficients of Aerosols," Appl. Opt. 18, 1372-1375 (1979).

A5. Walton, W.H., and Prewett, W.C., Proc. Phys. Soc. London Sect. B 62, 341 (1949).

A6. Carlon, H.R., Anderson, D.H., Milham, M.E., Tarnove, T.L., Frickel, R.H., and Sindoni, I., "Infrared Extinction Spectra of Some Common Liquid Aerosols," Appl. Opt. 16, 1598-1605 (1977).

APPENDIX B

MASS EXTINCTION COEFFICIENTS ESTIMATED FOR NONABSORBING SPHERICAL AEROSOL PARTICLES IN THE GEOMETRIC SCATTERING REGIME

The Beer-Lambert equation for aerosols can be written

$$- \ln T_\lambda = \alpha_\lambda C L, \qquad (B1)$$

where T_λ is the optical transmittance at wavelength λ (μm), α_λ is the mass extinction coefficient ($m^2\ g^{-1}$), C is the aerosol mass concentration ($g\ m^{-3}$), and L is the optical path length (m). It is straightforward to show[B1] that

$$\alpha_\lambda = 3Q_\lambda / 2D_\mu \rho, \qquad (B2)$$

where the Mie theory[B2] gives the value of Q_λ that depends on the particle diameter D_μ (μm) compared to wavelength λ, and ρ is the particle mass density ($g\ cm^{-3}$). In the geometric regime ($D_\mu \gg \lambda$), $Q_\lambda \rightarrow 2.0$ as D_μ increases. Thus,

$$\alpha_\lambda \rightarrow 3/D_\mu \rho. \qquad (D_\mu \gg \lambda) \qquad (B3)$$

For example, Figure B1 shows values of α_λ vs D_μ at the He:Ne laser wavelength ($\lambda = 0.63\ \mu m$) calculated for spherical droplets of water (dashed curve[B3]) and several phthalates (dibutyl, diethyl, dimethyl, dioctyl- solid curves); the latter are commonly used in aerosol chamber testing.[B4]

The figure shows that when $D_\mu \gg 0.63\ \mu m$, the Mie-calculated extinction coefficient curves merge into a tail whose function is given by Equation (B3) and whose thickness depends mainly on the differences in mass densities (ρ) of the liquids represented. The density differences are not obvious because of the logarithmic scale used for the ordinate of Figure B1.

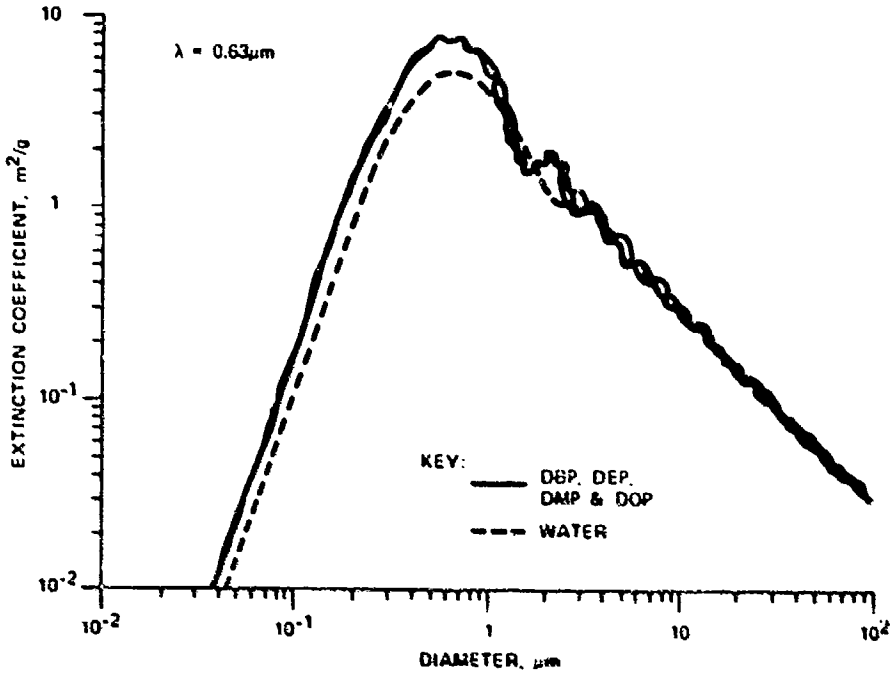

Figure B1. Mie-Calculated Extinction Coefficient vs Spherical Droplet Diameter for the He:Ne Wavelength (λ = 0.63 μm); the Dashed Curve Is for Water Droplets, While the Solid Curves Are for Droplets of Phthalates (Dibutyl, Diethyl, Dimethyl and Dioctyl).

A great many liquid and solid substances exist for which, when they are dispersed as spherical particles at wavelengths where their absorption is negligible, remarkably good first approximations of α_λ can be made using Equation (B3). Hence this equation is useful for first calculations involving such aerosols when their optical properties are not known at some wavelength λ, but $D_\mu >> \lambda$. A common example is that of water fog droplets in the visible wavelengths. Often, visible-wavelength observations can be combined with IR measurements to yield additional information about an aerosol, e.g., mean particle diameter.[B5] Combining Equations (B1) and (B5) gives

$$- \ln T_\lambda = 3CL/D_\mu \rho, \qquad (D_\mu >> \lambda) \qquad (B4)$$

and it is straightforward to show that

$$- \ln T_\lambda = \frac{\pi}{2}(D_\mu^2 \, NL \times 10^{-6}), \qquad (D_\mu >> \lambda) \qquad (B5)$$

where N is the number of spherical particles per cubic centimeter. Equation (B5) can be extended to some rather practical applications. For example, Middleton[B6] estimates meteorological range as that for which a high-contrast target is seen with 2% transmittance, i.e., $T_\lambda = 0.02$ and $- \ln T_\lambda = 3.912$, so that from Equation (B5)

$$N = (2.49 \times 10^6)/D_\mu^2 \, L. \qquad (D_\mu >> \lambda) \qquad (B6)$$

As an example, a typical developing water fog is comprised of droplets having mean diameters in the 3-5 μm range. If an observer could barely see a high-contrast target at L = 200 m under such conditions, from Equation B6 the fog should contain approximately 500-1400 droplets cm^{-3}. Perhaps a more useful application would be to calculate mean values of D_μ from Equation (6) using observed ranges (L) and droplet populations (N) measured by independent means, as a water fog aged and dissipated.

LITERATURE CITED

B1. Carlon, H.R., "Practical Upper Limits of the Optical Extinction Coefficients of Aerosols," Appl. Opt. 18, 1372-1375 (1979).

B2. Mie., G., Ann. Phys. Leipzig 25, 377 (1908).

B3. Carlon, H.R., Anderson, D.H., Milham, M.E., Tarnove, T.L., Frickel, R.H., and Sindoni, I., Infrared Extinction Spectra of Some Common Liquid Aerosols," Appl Opt. 16, 1598-1605 (1977).

B4. Carlon, H.R., Kimball, D.V., and Wright, R.J., "Laser Monitoring of Mass Concentrations of Monodisperse Test Aerosols," Appl. Opt. 19, 2366-2369 (1980).

B5. Carlon, H.R., Milham, M.E., and Frickel, R.H., "Determination of Aerosol Droplet Size and Concentration from Simple Transmittance Measurements," Appl. Opt. 15, 2452-2456 (1976).

B6. Middleton, W.E.K., Vision Through the Atmosphere, Univ. of Toronto Press, Toronto, 1952, p. 105.